Bull. Mater. Sci., Vol. 37, No. 2, April 2014, pp. 199–206. © Indian Academy of Sciences.

Ciprofloxacin conjugated zinc oxide nanoparticle: A camouflage towards multidrug resistant bacteria

PRASUN PATRA[a,*], SHOUVIK MITRA[a], NITAI DEBNATH[a], PANCHANAN PRAMANIK[b] and ARUNAVA GOSWAMI[a]

[a]AERU, Biological Sciences Division, Indian Statistical Institute, Kolkata 700 108, India
[b]Department of Chemistry, Indian Institute of Technology, Kharagpur, Kharagpur 721 302, India

MS received 23 March 2012; revised 1 October 2012

Abstract. **Gradual development of antibiotic resistant bacteria is producing severe global threat. Newer strategies are now being employed in order to control the microbial infections and to reduce the mortality as well as infection rates. Herein we describe successful synthesis of ZnO nanoparticles (ZNP) under microwave assisted condition followed by functionalization with ciprofloxacin, an antibiotic, using EDC/NHS chemistry. Successful conjugation of ciprofloxacin was confirmed by FTIR spectra. Ciprofloxacin-conjugated ZnO nanoparticles (ZN-CIP) exhibited excellent antibacterial activity against clinically isolated multidrug resistant bacterial strains of *Escherichia coli, Staphylococcus aureus* and *Klebsiella* sp. ZNP were small in size with particle size distribution 18–20 nm as obtained from transmission electron microscope (TEM). Surface topology was obtained from atomic force microscopic (AFM) image and x-ray diffraction confirmed that ZNP possessed hexagonal crystal structure. A concentration of 10 μg/mL of ZN-CIP was a benchmark concentration. During evaluation of minimum inhibitory concentration (MIC) values, similar concentration of antibiotic was incapable of producing antibacterial activity.**

Keywords. **Zinc oxide nanoparticles; ciprofloxacin; chemical conjugation; antibacterial property.**

1. Introduction

Gradual development of antibiotic resistant bacteria is producing severe global threat. Pathogenic species of *Escherichia coli*, *Staphylococcus aureus* and *Klebsiella* sp. are the common examples of such bacteria that cause a variety of infectious diseases worldwide. Recently in 2011, many people died in Germany due to severe infection caused by *E. coli* (BBC News, 1 June 2011) *Staphylococcus* is very well known for wide spectrum of phylogenic infections (Blanc *et al* 2000); meanwhile *Klebsiella* sp. can lead to a wide range of disease states, notably pneumonia, urinary tract infections, septicemia, ankylotic spondylitis and soft tissue infections. Newer strategies are now being employed in order to control the microbial infections and to reduce the mortality as well as infection rates (Saha *et al* 2007; Turos *et al* 2007; Chakraborty *et al* 2010). Rapid advance in nanotechnology offers researchers to apply diverse nanomaterials against biocidal applications. Nanoparticles of TiO_2, ZnO, silver, etc. are commonly known for their biocidal efficacy. ZnO is one of the five compounds identified as GRAS (generally recognized as safe) by US food and drug administration (Mitra *et al* 2012). Therefore, in this study we have exploited a safe nanomaterial fabricated with antibiotic towards antibiotic resistant bacteria to minimize the infectious effect.

ZnO nanoparticle (ZNP), with its versatile potential and multifunctional application, has grown to be one of the most promising nanomaterials. ZNP, with its band gap of 3·37 eV and a large excitation binding energy of 60 meV, can exhibit near ultraviolet emission and transparent conductivity. Wide applications of ZNP includes its use in cosmetics, medicine and drug delivery. ZNP is widely used in biosensors (Ren *et al* 2009), electrodes (Ku and Wu 2007), biogenerators (Wang and Song 2006), solar cells (Lee *et al* 2008), acoustic devices (Chivukula *et al* 2010), luminescent devices (Yude *et al* 2006) and in catalysis (Li *et al* 2009). Recently numerous works have been done on antimicrobial activity especially onantibacterial activity (Reddy *et al* 2007; Padmavathy and Vijayaraghavan 2008). Antibacterial activity of ZnO doped in silica matrix was observed against *E. coli* (Dutta *et al* 2010). Applerot *et al* (2009) proposed that formation of reactive oxygen species was the formal mechanism behind the damage of microbial system. Ciprofloxacin is one of the most significant antibiotics used in medicinal sector. Therefore, conjugation of antibiotic with a nanoparticle is expected to increase its efficacy. We have chosen ZNP to conjugate with antibiotic as ZnO, which is biosafe and biocompatible and can be used for biomedical application without coating (Wang 2004). Banoee *et al* (2010) have reported that mixture of zinc oxide and ciprofloxacin is effective against bacterial system. However, no reports are still available on antibacterial activity of chemically conjugated ciprofloxacin against multidrug resistant bacteria to best of our knowledge.

Herein we describe successful synthesis of ZNP under microwave assisted condition followed by fabrication of ZNP with an antibiotic ciprofloxacin. ZNP was then amine

*Author for correspondence (bioprasun@gmail.com)

functionalized by using a silane coupling agent APTES (3-aminopropyltriethoxysilane) under refluxing condition using dimethyl sulphoxide as the solvent. Ciprofloxacin was then conjugated with ZNP using EDC/NHS chemistry to produce ciprofloxacin conjugated zinc oxide nanoparticle (ZN-CIP). Successful chemical conjugation was confirmed by UV–Vis and FTIR spectra. ZN-CIP exhibited brilliant antibacterial activity against clinically isolated multidrug resistant bacteria with dose dependency.

2. Experimental

2.1 *Materials*

Zinc acetate dihydrate, tris(hydroxymethyl)aminomethane, dimethyl sulfoxide, ethanol and 3-ethyldimethylaminopropyl carbodiimide (EDC) were purchased from Merck (India), N-hydroxysuccinimide (NHS) was purchased from SRL (India), 3-aminopropyltriethoxysilane was purchased from Sigma Aldrich and Muller Hilton broth was obtained from Himedia. All the chemicals were of analytical grade and used without further purification. Milli-Q grade water (Sartorious Stedim Biotech) was used throughout the experiment with conductivity less than 0·1 μS cm^{-1}.

2.2 *Synthesis of ZnO nanoparticle*

Most of the reported methods involve synthesis of zinc oxide under strong alkaline and drastic conditions. But, we have used TRIS buffer providing milder conditions. In brief, 20 ml 20% aqueous TRIS solution was added drop wise to 25 ml of 0·05(M) zinc acetate dihydrate solution. The mixture was stirred well and then subjected to microwave irradiation at 300 watt for 3 min in a domestic microwave. The obtained product was centrifuged at 10000 rpm for 10 min and washed several times with milli-Q water in order to remove excess of TRIS buffer. Finally, the product was washed with ethanol and dried overnight at 80 °C in a hot air oven.

2.3 *Amine functionalization of ZnO nanoparticle*

Amine functionalization of ZNP was carried out by using 3-aminopropyltriethoxysilane via co-condensation reaction with modification of the reported method (Guo *et al* 2009). In brief, about 0·5 g of ZNP was dispersed in about 50 mL of DMSO in a sonication bath for about 1 h. The resultant dispersion was transferred to a round bottom flask attached with a reflux condenser. To it 400 μL of 3-APTES was added and the solution was refluxed at 120 °C for about 3 h. After completion of the reaction, the resulting nanoparticle was centrifuged at 12000 rpm for about 15 min and washed several times with ethanol to remove the unreacted 3-APTES. Finally, the product was dried at 60 °C overnight to produce amine functionalized ZNP.

2.4 *Conjugation of ciprofloxacin with ZnO nanoparticles*

Ciprofloxacin was chemically conjugated with amine functionalized ZNP using EDC/NHS chemistry. Briefly, 15 mg of ciprofloxacin was dispersed by sonication in 30 mL 1:1 aqueous DMSO. To it, 8 mg of EDC was added followed by the addition of 8 mg of NHS. pH of the system was maintained at 6. The mixture was allowed to stir for 3 h in a dark atmosphere. After activation of ciprofloxacin, 30 mg of amine functionalized ZNP dispersed in 10 mL of 1:1 aqueous DMSO was added dropwise. pH was maintained at 8 and the reaction mixture was allowed to stir overnight. Then, ZN-CIP was obtained by centrifugation of the reaction mixture at 4000 rpm for about 15 min and washed a few times with DMSO and ethanol. Finally obtained ZN-CIP was dried at 60 °C.

2.5 *Antibacterial assay*

Multi drug resistant (resistant to ciprofloxacin, ofloxacine, tetracycline, chloramphenicol and gintamicin) pathogenic bacterial strains of *E. coli*, *Staphylococcus aureus* and *Klebseilla* sp. were isolated from clinical specimens (urine, throat swab and pus) which were grown in Muller Hilton broth medium at 37 °C temperature under aerobic conditions. Strains were routinely cultured overnight at 37 °C with agitation in MH broth. At experimental phase, bacteria were harvested by centrifugation at 3000 rpm for 10 min and washed twice with phosphate buffer saline (PBS, pH 7·2) and then resuspended in PBS. The bacterial concentration was adjusted to 1 $\times$ 10^6 CFU/mL by using the optical density (OD) of bacterial suspension.

Then 50 μL of inocula (1 $\times$ 10^6 CFU/mL) were added to 5 mL of Muller Hilton broth followed by addition of ZN-CIP dispersions of concentration of 1, 2, 5, 10, 20, 40, 60, 80, 160, 320, 500 and 1000 μg/mL with respect to total volume of 5 mL. Finally, autoclaved deionized water was added to make up the volume 5 mL of each test tube. The dispersions were cultured at 37 °C with gentle stirring. In liquid medium, the growth of bacterial strains was indexed by measuring OD at 600 nm against abiotic control using UV–Vis spectrophotometer (Dutta *et al* 2010).

2.6 *Bacterial cell membrane damage assay*

Damaged bacterial membrane would release cytoplasmic constituents of the cell which can be monitored easily. Release of DNA and RNA from cytoplasm can be monitored by measuring the absorbance at 260 nm. The experiment was conducted as follows. The bacterial suspension (here *E. coli*) was separated into several flasks. Then ZNP, CIP and ZN-CIP of concentration 20 μg/mL were added in separate flasks. Samples of 1·5 mL were removed from the flasks every 1 h, and immediately filtered through 0·2 μm syringe filter to remove the bacteria. The supernatant was

then diluted appropriately and optical density was recorded at 260 nm.

3. Characterization

Morphology was investigated using field emission scanning electron microscope (FESEM) of Carl Zeiss (Germany) with acceleration voltage of 5·0 kV. For FESEM alcoholic dispersion of ZNP was put on a properly cleaned glass slide followed by spin coating. Ultraviolet–Visible (UV–Vis) spectra of the sample were carried out using a Shimadzu (Singapore) absorption spectrophotometer (Model No. 1700), a photoluminescence (PL) spectrum was recorded in Hitachi spectrofluorimeter (model no: F-7000). X-ray diffraction (XRD) pattern of the sample was carried out in a PANalytical X-PERT PRO (USA), applying a primary beam monochromator to select the Kα1 component of the employed copper radiation (wavelength of 1·54056 Å). Fourier transform infrared spectroscopy (FTIR) was recorded in Perkin-Elmer (USA) spectrum 100. Prior to FTIR measurements, the samples were ground with KBr (spectroscopic grade) and pressed to pellets. Atomic force microscopy (AFM) was carried out using an NT-MDT (NTEGRA, Netherland). For AFM, a sample solution, diluted in ethanol, was drop casted in a properly cleaned glass slide and well dried in air. AFM was carried out in tapping mode. Particle size was determined by using transmission electron microscope (TEM) of Phillips CM 200 (Netherlands) at an operational voltage of 200 kV. For TEM micrograph, a well dispersed solution of the sample in ethanol was put into uniform carbon coated copper TEM grid and well dried in vacuum. For antibacterial efficacy OD of the samples were measured by using the same UV–Vis spectrometer with determination of minimum inhibitory concentration (MIC) and the results were analyzed statistically.

4. Results and discussion

4.1 *Physicochemical characterizations*

Herein we describe successful chemical conjugation of an antibiotic with ZNP and its application against drug resistant bacteria. Figure 1 shows the schematic representation of the whole process. ZNP were synthesized by a microwave assisted process from the zinc precursor, zinc acetate dihydrate, followed by its amine functionalization using 3-APTES. Carboxylic acid group of the antibiotic was utilized in course of chemical conjugation with amine functionalized ZNP using EDC/NHS chemistry.

Preliminary investigation by UV–Vis spectra justified chemical conjugation of ciprofloxacin with ZNP. Figure 2

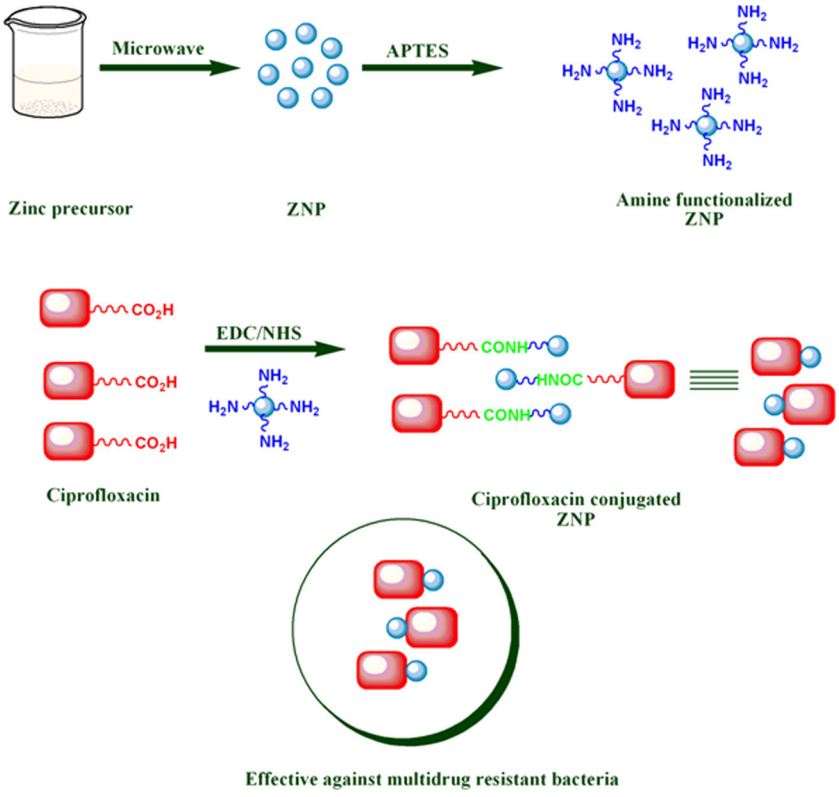

Figure 1. Schematic representation illustrating the whole process of chemical conjugation of ciprofloxacin with zinc oxide nanoparticles.

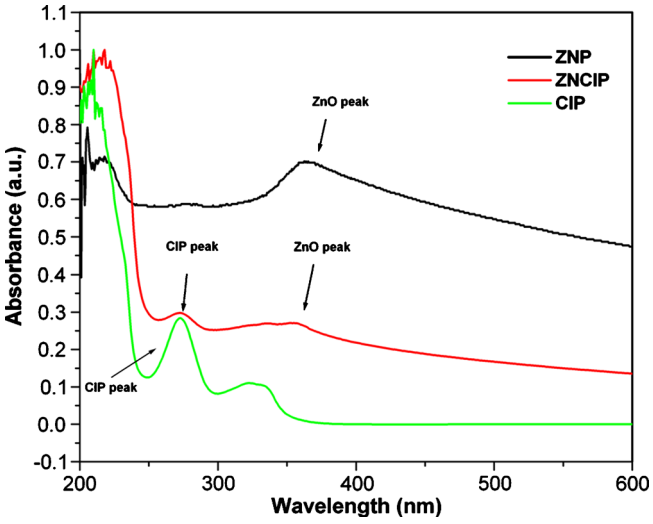

Figure 2. UV–Vis absorbance spectra of zinc oxide nanoparticles (ZNP), ciprofloxacin (CIP) and zinc oxide chemically conjugated with ciprofloxacin (ZN-CIP).

shows the UV–Vis spectra of all the three components. ZNP synthesized by microwave assisted process exhibited a steep peak at 363 nm and it was again a characteristic peak of ZNP (Bhattacharyya and Gedanken 2008) as reported by other processes. Meanwhile, native ciprofloxacin exhibited two characteristic peaks — one at 326 nm and other at 272 nm. After conjugation with ZNP, though the second peak did not shift, the first one slightly shifted to 336 nm with a new peak at 357 nm corresponding to ZNP.

Successful conjugation was confirmed by FTIR spectra as shown in figure 3. Figure 3 (blue line) represents the FTIR spectra of ZNP in which characteristic peaks at 3400 cm^{-1}, 1632 cm^{-1} and lower bands justified O–H, C=O (carbonyl) and Zn–O (Zhang *et al* 2010) stretching, respectively. The peaks obtained in the region of 1400 cm^{-1} and 1462 cm^{-1} were pertinent to O–H and N–H bending, though the amount of N–H group was less. The red line represents FTIR spectra of amine functionalized ZNP. It shows a characteristic peak at 3373 cm^{-1} due to the presence of O–H stretching frequency along with –N–H stretching frequency of NH_2 group. Peaks obtained at 2930 cm^{-1} were due to the asymmetric C–H stretching frequency of the CH_2 group coming from APTES fragment. Two small distinct peaks at 1580 cm^{-1} and 1470 cm^{-1} were attributed towards NH_2 scissoring of primary amine. A small distinct peak at 1411 cm^{-1} signified –O–H bending with a lower intensity. Two additional sharp peaks at 1020 cm^{-1} and 1117 cm^{-1} suggested Si–O and C–N stretching, respectively. The lower wave number band was attributed to characteristic Zn–O stretching. The green line in figure 3 represents the FTIR spectra of ZN-CIP. Peaks obtained at 3420 cm^{-1}, 2930 cm^{-1} justified O–H and C–H stretching, respectively, whereas the amide doublet was observed at 1652 cm^{-1} and 1560 cm^{-1} (Das *et al* 2009). Corresponding O–H bending was shifted to 1398 cm^{-1}, while the other bands signifying Si–O and C–N stretching was

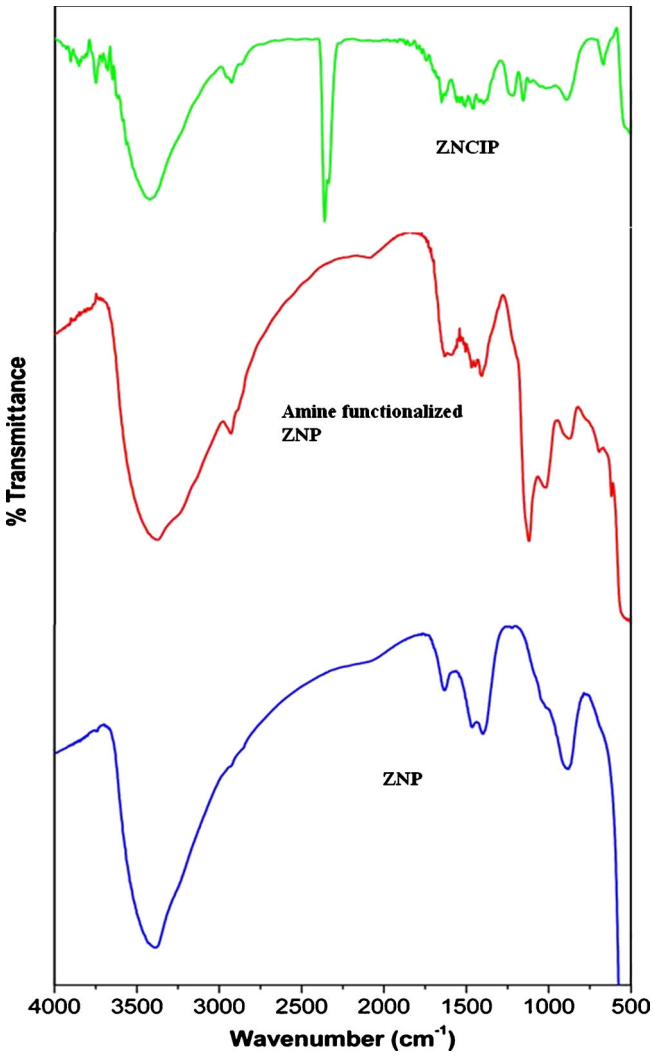

Figure 3. FTIR spectra of zinc oxide nanoparticles (blue line), amine functionalized zinc oxide nanoparticles (red line) and zinc oxide nanoparticles chemically conjugated with ciprofloxacin (green line).

shifted to 1118 cm^{-1} and 1229 cm^{-1}, respectively. Small peaks obtained in the region of 1400–1550 cm^{-1} were similar to ciprofloxacin peaks, while 890 cm^{-1} signified Zn–O stretching frequency and the lowest wave number band was again the characteristic peak of ciprofloxacin and ZnO nanoparticle, respectively.

Powder XRD of ZNP exhibited ten characteristic peaks with 2θ = 31·60°, 34·21°, 36·02°, 47·37°, 56·51°, 62·76°, 66·15°, 67·70°, 68·89° and 76·85° which could easily be indexed to (100), (002), (101), (102), (110), (103), (200), (112), (201) and (202) diffraction planes with hexagonal structure [JCPDS card no. 034477] (Sharma *et al* 2010). XRD diffraction pattern is depicted in figure 4(a). No additional peaks were obtained in the diffraction pattern which suggested its chemical purity. PL property of ZN-CIP is shown in figure 4(b). Two PL peaks were obtained when it was excited at 340 nm. The first one was the sharp one centering at 383 nm, while the broad second one was centered

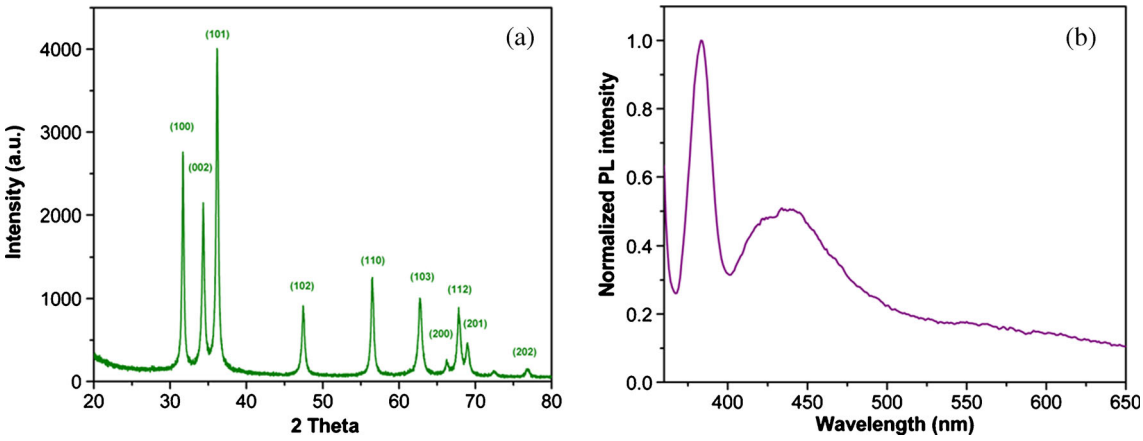

Figure 4. (**a**) XRD pattern of zinc oxide nanoparticles and (**b**) PL spectra of ciprofloxacin conjugated zinc oxide nanoparticles.

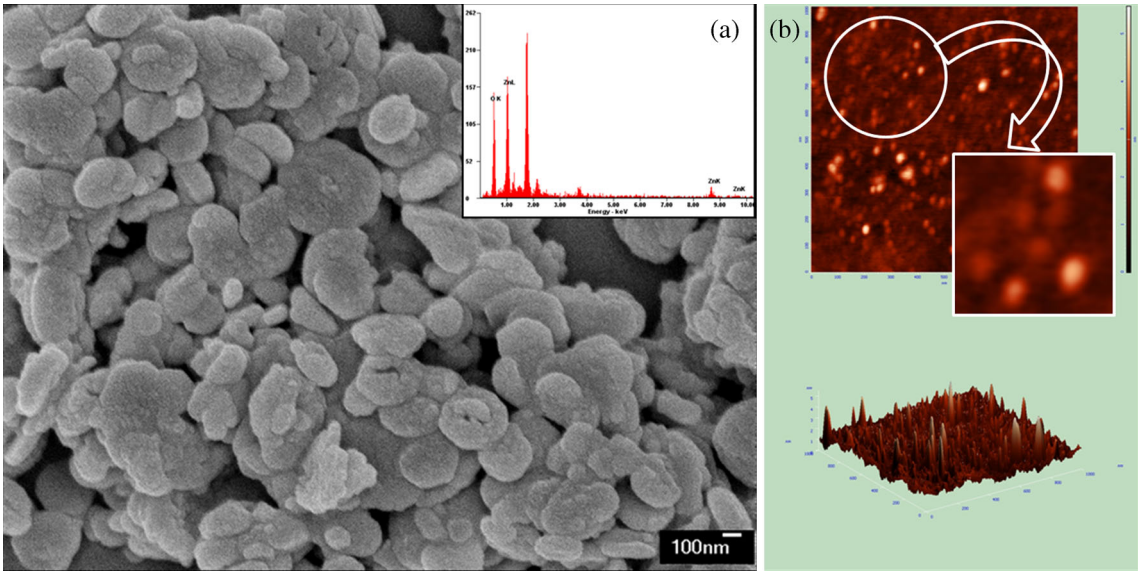

Figure 5. (**a**) FESEM image of ZNP and inset indicating its EDX spectrum and (**b**) atomic force microscopic 2D and 3D image respectively.

at 438 nm. This pattern was identical as obtained by Pandey *et al* (2010), but due to chemical conjugation with ciprofloxacin the peaks were shifted to a lower wavelength. Among the bands, the lower was attributed to the recombination of excitons (Vanheusden *et al* 1996) while the broad peak could be indexed to singly ionized oxygen vacancy in ZnO, resulting from the recombination of a photon-generated hole with the single ionized charge state of defect (Monticone *et al* 1998).

Morphology of synthesized ZNP from FESEM is shown in figure 5(a), which showed that the particles were partly spherical in nature and similar morphologies were maintained throughout. An EDX spectrum was carried out by drop casting of the sample followed by spin coating which showed Zn and O were the main chemical components. The EDX spectrum is shown in figure 5(a) inset. Zinc oxide and other semiconductor materials might be important for providing antimicrobial functionality to next generation medical devices. AFM images revealed that the particles were more or less spherical in nature. AFM image is shown in figure 5(b). AFM image also justified distribution of spherical particles.

However, the appropriate particle size was measured from HRTEM analysis which is shown in figure 6. TEM micrograph justified that the ZNP were small in size, ranging from 18 to 20 nm, though they were agglomerated to some extent and most of them were spherical in nature. Corresponding SAED pattern is shown in figure 6 inset which

justified its crystalline structure. This agglomeration for ZNP was expected with other TEM micrograph obtained by Bauermann *et al* (2006) via different synthetic route.

4.2 *Antibacterial effect of ZN-CIP*

Antibiotics were found to be a valuable weapon to combat bacterial infection, but their popularity had also become their undoing. Although the drugs crippled harmful microbes from within, bacteria that survived such sabotage tend to develop resistance that made them even more dangerous. Drug resistance developed in part because conventional antibiotics such as ciprofloxacin and doxycycline did not physically damage a microbe's cell wall. Instead, they entered their target less disruptively and moved on to disrupt the DNA within or block cell division or trigger cellular self-destruction. Strains that survived this assault, however, could evolve to defend themselves against future attacks, opened the door for deadlier versions of bacteria such as methicillin-resistant *Staphylococcus aureus* (MRSA), which killed nearly 19,000 Americans in 2005. To counter this, we have developed ZN-CIP to supplement pure antibiotics by destroying outer protective membranes of bacteria, ensuring that their morphing days are through.

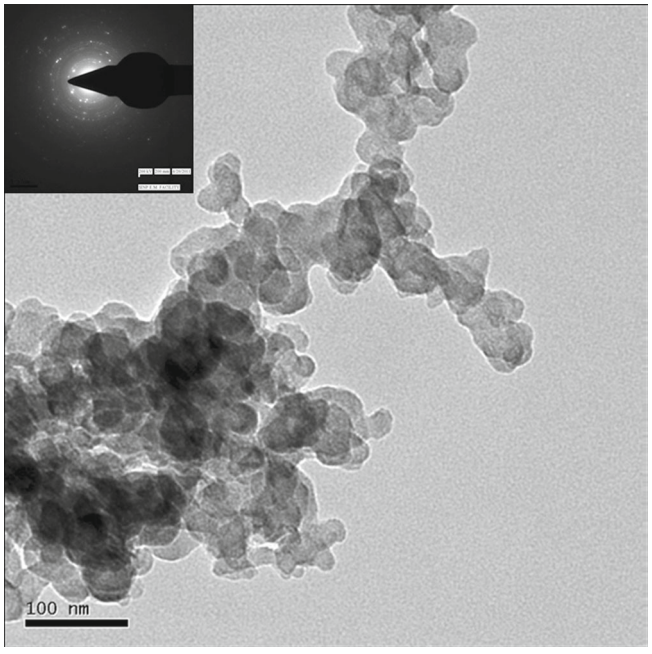

Figure 6. HRTEM image of ZNP (inset showing its SAED pattern).

Successful efficacy was observed by using ZN-CIP with dose dependency. Partial growths of bacterial strains were visible up to 10 μg/mL of ZN-CIP concentration, but no growths were visible at 20 μg/mL of ZN-CIP concentration. Therefore, MIC value was found to be 20 μg/mL for ZN-CIP. Meanwhile, two other antibiotics — norfloxacin and ciprofloxacin — were unable to restrict the growth of bacterial strains at similar concentration. Dose dependency bars against concentration is illustrated in figure 7. It showed that, when ciprofloxacin was conjugated with ZNP, the conjugated system was successfully able to produce an overwhelming response against multidrug resistant bacteria. Here ZNP damaged the cell membrane through reactive oxygen species (ROS) generation with free electrons and holes in presence of light (Jang *et al* 2006), which assisted ciprofloxacin to enter into the cell and, thereby, inhibit bacterial growth. Again ZNP were known to be abrasive due to surface defects (Stoimenov *et al* 2002), which could contribute to the mechanical damage of the cell membrane of bacteria to some extent as well. Even Wang *et al* (2007) proposed that the orientation of ZnO

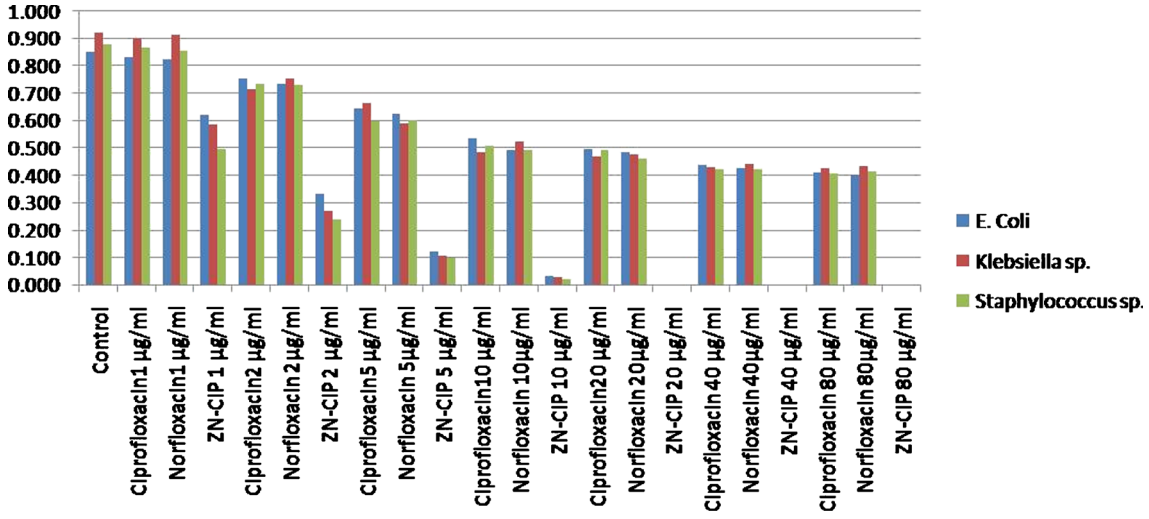

Figure 7. Estimation of MIC value of ZN-CIP against multi drug resistant clinically isolated strains of *E. coli*, *S. aureus* and *Klebsiella* sp. along with norfloxacin and ciprofloxacin at the concentration.

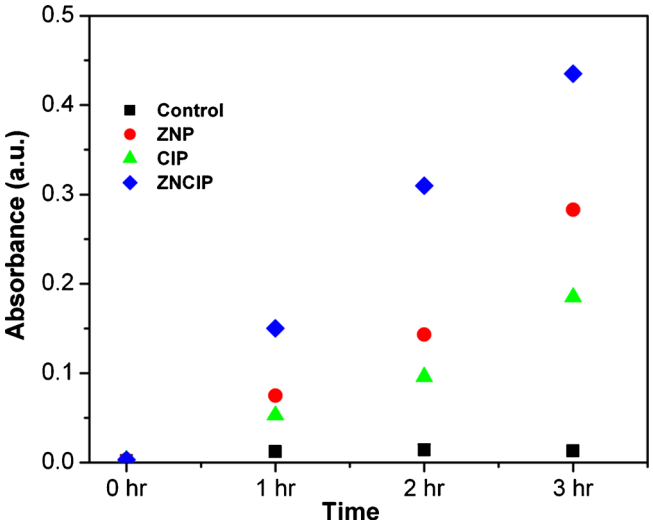

Figure 8. Mean absorbance against time to study release of cytoplasm material (DNA and RNA) from Control, ZNP, CIP and ZN-CIP treated *E. coli* at 260 nm at 0, 1, 2 and 3 h time intervals.

can also affect outer surface of bacteria. Cell membrane damage was confirmed by 260 nm release assay (Chen and Cooper 2002). Release of substances such as DNA, RNA and other materials was the indicator of the integrity of the cell membrane of bacteria. Any disruption in cell membrane would lead to leakage of these substances. Hence, absorbance at 260 nm would increase accordingly. Figure 8 shows that the absorbance at 260 nm was maximum at MIC value of ZN-CIP. This could be due to the combined effect of ZNP and ciprofloxacin resulting in maximum damage of cell membrane leading to the death of bacteria in contrast to ZNP and ciprofloxacin alone.

5. Conclusions

In conclusion, we have reported a microwave assisted synthesis of ZNP using a buffer which is nontoxic to a wide variety of biological systems and provided an enhanced buffering capacity (Good *et al* 1966) under a mild reaction condition. ZNP attained hexagonal crystal structure and TEM images justified its small size distribution of 18–20 nm. ZNP were chemically conjugated with ciprofloxacin and successful chemical conjugation was confirmed by FTIR spectra. ZN-CIP exhibited enhanced bactericidal activity against multi drug resistant clinically isolated strains of *E. coli*, *S. aureus* and *Klebsiella* sp. with dose dependency. A concentration of 10 μg/mL of ZN-CIP was a benchmark concentration during evaluation of MIC values. Similar concentration of antibiotic was incapable of producing antibacterial activity. The roughness of native ZNP of ZN-CIP, together with ROS, damaged the bacterial cell membrane allowing the antibiotic conjugated ZN-CIP to penetrate into the cell and disrupt cell division which is not possible with the antibiotic alone.

Acknowledgement

The authors would like to thank DBT-GOI, ICAR-NAIP, ICAR-National Fund, and ISI Plan Project 2011–2014 for their generous financial support. SM is thankful to CSIR for their financial assistance.

References

Applerot B G, Lipovsk A, Dror R, Perkas N, Nitzan Y, Lubart R and Gedanken A 2009 *Adv. Funct. Mater.* **19** 842

Banoee M, Seif S, Nazari Z E, Fesharaki P J, Shahverdi H R, Moballegh A, Moghaddam K M and Shahverdi A R 2010 *J. Biomed. Mater. Res. B* **93B** 557

Bauermann L P, Bill J and Aldinger F 2006 *J. Phys. Chem. B* **110** 5182

BBC News 1 June 2011 (http://www.bbc.co.uk/news/world-europe-13613487)

Bhattacharyya S and Gedanken A 2008 *Micropor. Mesopor. Mat.* **110** 553

Blanc D S, Banuls A L, Hauser P M, Moreillon P, Francioli P and Tibayrenc M 2000 *Microb. Drug Resist.* **6** 231

Chakraborty S P, Sahu S K, Mahapatra S K, Santra S, Bal M, Roy S and Pramanik P 2010 *Nanotechnology* **21** 105103

Chen C Z and Cooper S L 2002 *Biomater.* **23** 3359

Chivukula V, Ciplys D, Shur M and Dutta P 2010 *Appl. Phys. Lett.* **96** 233512

Das M, Mishra D, Dhak P, Gupta S, Maity T K, Basak A and Pramanik P 2009 *Small* **24** 2883

Dutta R K, Sharma P K, Bhargava R, Kumar N and Pandey A C 2010 *J. Phys. Chem. B* **114** 5594

Good N E, Winget G D, Winter W, Connolly T N, Izawa S and Singh R M M 1966 *Biochemistry* **5** 467

Guo Y, Wang H, He C, Qiu L and Cao X 2009 *Langmuir* **25** 4678

Jang Y J, Simer C and Ohm T 2006 *Mater. Res. Bull.* **41** 67

Ku C H and Wu J J 2007 *Nanotechnology* **18** 505706

Lee Y J, Ruby D S, Peters D W, McKenzie B B and Hsu J W P 2008 *Nano Lett.* **8** 1501

Li S F, Zhang X M, Du W X, Ni Y H and Wei X W 2009 *J. Phys. Chem. C* **113** 1046

Mitra S, Chandra S, Laha D, Patra P, Debnath N, Pramanik A, Pramanik P and Goswami A 2012 *Mater. Res. Bull.* **47** 586

Monticone S, Tufeu V and Kanaev A V 1998 *J. Phys. Chem. B* **102** 2854

Padmavathy N and Vijayaraghavan R 2008 *Sci. Technol. Adv. Mater.* **9** 035004

Pandey A C, Sanjay S S and Yadav R S 2010 *J. Exp. Nanoscience* **5** 488

Reddy K M, Feris K, Bell J, Wingett D G, Hanley C and Punnoose A 2007 *Appl. Phys. Lett.* **90** 213902

Ren X, Chen D, Meng X, Tang F, Hou X, Han D and Zhang L 2009 *J. Colloid Interface Sci.* **334** 183

Saha B, Bhattacharya J, Mukherjee A, Ghosh A K, Santra C R, Dasgupta A K and Karmakar P 2007 *Nanoscale Res. Lett.* **2** 614

Sharma D, Rajput J, Kaith B S, Kaur M and Sharma S 2010 *Thin Solid Films* **519** 1224

Stoimenov P K, Klinger R L, Marchin G L and Klabunde K J 2002 *Langmuir* **18** 6679

Turos E, Shim J Y, Greenhalgh K, Reddy G S, Dickey S and Lim D V 2007 *Bioorg. Med. Chem. Lett.* **17** 53
Vanheusden K, Warren V, Seager C H, Tallant D R, Voigt J A and Gnade B E 1996 *J. Appl. Phys.* **79** 7983
Wang X, Yang F, Yang W and Yang X 2007 *Chem. Commun.* **42** 4414
Wang Z L 2004 *Materials Today* **7** 26
Wang Z L and Song J H 2006 *Science* **312** 242
Yude W, Shuo Z, Xinghui W and Qingju L 2006 *Mater. Chem. Phys.* **98** 121
Zhang B, Kong T, Xu W, Su R, Gao Y and Cheng G 2010 *Langmuir* **26** 4514